

Absence of magnetic long range order in Y_2CrSbO_7 : bond-disorder induced magnetic frustration in a ferromagnetic pyrochlore

L. Shen,¹ C. Greaves,² R. Riyat,¹ T. C. Hansen,³ and E. Blackburn¹

¹*School of Physics and Astronomy, University of Birmingham, Birmingham B15 2TT, United Kingdom*

²*School of Chemistry, University of Birmingham, Birmingham B15 2TT, United Kingdom*

³*Institut Laue-Langevin, BP 156, 38042 Grenoble Cedex 9, France*

The consequences of nonmagnetic-ion dilution for the pyrochlore family $Y_2(M_{1-x}N_x)_2O_7$ (M = magnetic ion, N = nonmagnetic ion) have been investigated. As a first step, we experimentally examine the magnetic properties of Y_2CrSbO_7 ($x = 0.5$), in which the magnetic sites (Cr^{3+}) are percolative. Although the effective Cr-Cr spin exchange is ferromagnetic, as evidenced by a positive Curie-Weiss temperature, $\Theta_{CW} = 20.1(6)$ K, our high-resolution neutron powder diffraction measurements detect no sign of magnetic long range order down to 2 K. In order to understand our observations, we performed numerical simulations to study the bond-disorder introduced by the ionic size mismatch between M and N . Based on these simulations, bond-disorder ($x_b \simeq 0.23$) percolates well ahead of site-disorder ($x_s \simeq 0.61$). This model successfully reproduces the critical region ($0.2 < x < 0.25$) for the Néel to spin glass phase transition in $Zn(Cr_{1-x}Ga_x)_2O_4$, where the Cr/Ga-sublattice forms the same corner-sharing tetrahedral network as the M/N -sublattice in $Y_2(M_{1-x}N_x)_2O_7$, and the rapid drop in magnetically ordered moment in the Néel phase [Lee *et al.*, Phys. Rev. B 77, 014405 (2008)]. Our study stresses the nonnegligible role of bond-disorder on magnetic frustration, even in ferromagnets.

I. INTRODUCTION

Magnetic frustration, which often leads to interesting spin structures, refers to systems where the total free energy cannot be minimized by optimizing the interaction energy between each pair of spins¹. Magnetic interactions can be frustrated by geometry. For example, magnetic long range order is prohibited for the Heisenberg antiferromagnet on a triangular (or tetrahedral) lattice². The corresponding magnetic ground state, named spin liquid, is highly degenerate³⁻⁵. In addition to geometry, the competition between different types of magnetic interactions can also lead to magnetic frustration. The Ising rare-earth pyrochlores $R_2Ti_2O_7$ ($R = Ho, Dy$), in which the R -sublattice forms a corner-sharing tetrahedral network, develop a novel two-in/two-out spin ice structure due to the competing exchange and dipole-dipole interactions^{2,6,7}. Strikingly, the excited quasiparticles of a spin ice are found to resemble the behaviour of magnetic monopoles^{8,9}.

The effect of disorder has been widely investigated in magnetic materials and disorder is commonly used to generate spin glasses¹⁰. In general, a spin glass (SG) state prevails in systems dominated by randomness and frustration, which can be realized by either site- or bond-disorder.

Site-disorder arises when ions with different magnetic properties may be found randomly distributed on the same crystallographic sites, and is a very effective way to frustrate the Ruderman-Kittel-Kasuya-Yosida (RKKY) interaction. SG alloys such as Cu-Mn, Au-Mn and Au-Fe belong to this category^{11,12}. Moreover, SG can also be induced by diluting magnetic sites using nonmagnetic ions to pass the site-disorder percolation threshold (x_s), as in $Eu_{1-x}Sr_xS$ ($x_s \approx 0.136$)^{10,13}.

Bond-disorder arises due to randomization of bond-

length. Recent theoretical advances^{14,15} strongly suggest that bond-disorder is essential to generate a SG state in magnetic pyrochlores and spinels such as $Y_2Mo_2O_7$ ^{2,16-18} and $Zn(Cr_{1-x}Ga_x)_2O_4$ ¹⁹⁻²¹. In the latter compound, the SG is not related to the site-disorder since the onset composition of SG, $0.2 < x < 0.25$ ²¹, is well below the percolation threshold of the nonmagnetic Ga^{3+} -sites, $x_s \approx 0.61$ ²².

To the best of our knowledge, whether bond-disorder alone can lead to magnetic frustration remains to be unveiled. Although bond-disorder is decisive in $Y_2Mo_2O_7$ and $Zn(Cr_{1-x}Ga_x)_2O_4$ ^{14,15}, its influence on magnetic frustration is not clear due to the coexisting geometric frustration in these materials. Theoretically, it is argued that the weak bond-disorder acts as a perturbation to partially lift the degeneracy of a spin liquid¹⁴. From this point of view, bond-disorder does not facilitate magnetic frustration in systems composed of antiferromagnetically coupled spins. In addition, neither of the theories mentioned above could reproduce the critical region ($0.2 < x < 0.25$) for the Néel to SG phase transition in $Zn(Cr_{1-x}Ga_x)_2O_4$ ²¹.

To demonstrate the exclusive influence of bond-disorder on magnetic frustration, or in other words, to avoid geometric frustration, we have studied a series of diluted ferromagnetic transition-metal (TM) pyrochlores, $Y_2(M_{1-x}N_x)_2O_7$ (M = magnetic TM ion, N = nonmagnetic ion), where the yttrium-sites are nonmagnetic and bond-disorder is introduced by the ionic size mismatch between M and N . According to Ref. 22, we expect N -sites to percolate at $x_s \approx 0.61$. Specifically, we have employed $Y_2Mn_2^4O_7$ ²³ ($x = 0$) as the bond ordered start compound and $Y_2(Cr_{1-x}^{3+}Ga_x^{3+}Sb_{0.5}^{5+})_2O_7$ ($0.5 \leq x \leq 0.9$) as the bond disordered compounds. The magnetic TM ions in these systems (Mn^{4+} and Cr^{3+}) share the same electronic configuration ($3d^3$). Exper-

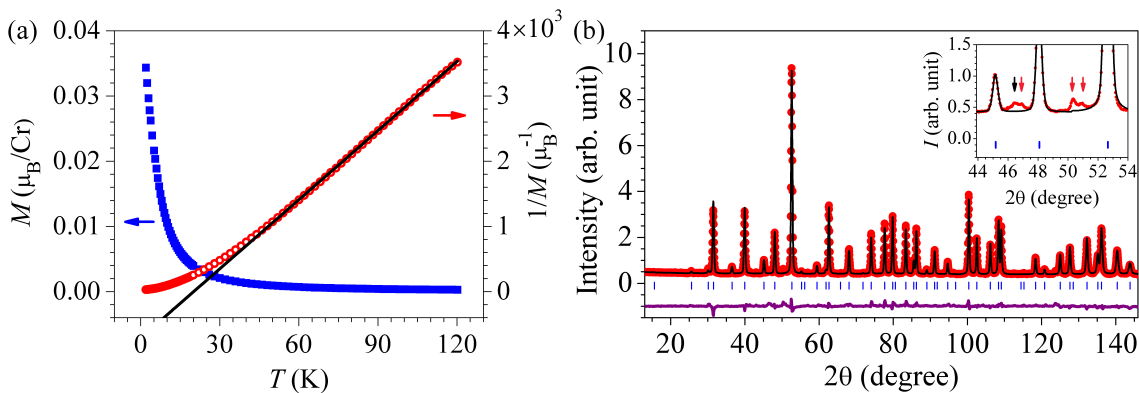


FIG. 1. (a) Temperature dependences of magnetization (left axis, blue solid squares) and inverse magnetization (right axis, red open circles) of Y_2CrSbO_7 measured at $\mu_0 H = 0.01$ T. The black solid line is a Curie-Weiss fit to the linear part of the $1/M$ - T curve in the paramagnetic region. (b) HRNPD pattern (red solids) of Y_2CrSbO_7 at $T = 2.0$ K, $B = 0$ T. Calculated pattern (black line), nuclear Bragg positions (blue vertical line) and difference (purple line) are also displayed. (inset) Enlarged version of a selected angle region. Additional peaks from YCrO_3 (red arrows) and the vanadium sample can (black arrow) can be seen.

imentally, we have performed magnetization and high-resolution neutron powder diffraction (HRNPD) measurements on $\text{Y}_2(\text{Cr}_{1-x}\text{Ga}_{x-0.5}\text{Sb}_{0.5})_2\text{O}_7$ ($0.5 \leq x \leq 0.9$). In Y_2CrSbO_7 ($x = 0.5 < x_s$), we find no evidence of zero-field magnetic long range order down to 1.8 K despite having a positive Curie-Weiss temperature $\Theta_{\text{CW}} = 20.1(6)$ K. Since Cr-sites are percolative in Y_2CrSbO_7 ²², site-disorder cannot be the driving mechanism of the observed high magnetic frustration. We have also carried out comprehensive numerical simulations to study the percolation processes of various nonmagnetic clusters, including bond-disorder, site-disorder, and the intermediate types in between (see Section III). Based on these simulations, bond-disorder percolates at $x_b = 0.23(1)$ on a pyrochlore lattice, pointing to the percolative bond-disorder in Y_2CrSbO_7 ($x = 0.5$). Our model also explains why the Néel to SG phase transition in $\text{Zn}(\text{Cr}_{1-x}\text{Ga}_x)_2\text{O}_4$ happens between $x = 0.2$ and 0.25 , as well as its rapid drop in magnetically ordered moment in the Néel phase upon Ga-substitution²¹. The nonnegligible role of bond-disorder in the zero-field magnetic frustration in Y_2CrSbO_7 is further supported by recovering the magnetic long range order at high magnetic fields.

II. EXPERIMENTS

Polycrystalline samples of $\text{Y}_2(\text{Cr}_{1-x}\text{Ga}_{x-0.5}\text{Sb}_{0.5})_2\text{O}_7$ ($0.5 \leq x \leq 0.9$) were synthesized by the solid-state reaction method in three steps²⁴. First of all, GaSbO_4 (CrSbO_4) powders were prepared by heating Ga_2O_3 (Cr_2O_3) (3N) and Sb_2O_3 (3N, 5% excess to compensate the volatilization) for 3 days at 640°C , and then 5 days at 1200°C with several intermediate regrindings. The intermediate temperature (640°C) is to transform Sb_2O_3 into Sb_2O_4 . To prepare Y_2GaSbO_7 (Y_2CrSbO_7), a stoichiometric mixture (1:1) of GaSbO_4

(CrSbO_4) and Y_2O_3 (4N) were heated in air for 6 days at 1200°C with several intermediate regrindings as well. Finally, $\text{Y}_2(\text{Cr}_{1-x}\text{Ga}_{x-0.5}\text{Sb}_{0.5})_2\text{O}_7$ was obtained by heating the stoichiometrically mixed Y_2GaSbO_7 and Y_2CrSbO_7 powders for 5 days at 1200°C .

Magnetization data were recorded using a Magnetic Property Measurement System (MPMS, Quantum Design). X-ray powder diffraction measurements were performed using a Bruker D8 diffractometer (Cu $K\alpha 1$, $\lambda = 1.5406 \text{ \AA}$) at room temperature. HRNPD patterns were collected at the D2B powder diffractometer ($\lambda = 1.594 \text{ \AA}$), equipped with a 5 T vertical cryomagnet, at the Institute Laue-Langevin (ILL) in Grenoble, France²⁵. For these measurements, about 8 g of each powder sample were hydraulically pressed into a cylinder (height = 11 mm, diameter = 13 mm) to avoid any field-induced texture and then loaded into a vanadium container. Rietveld refinements were carried out using the FullProf package²⁶.

An impurity phase, identified as YCrO_3 , with a volume fraction of $3.4(2)\%$, is necessary to match some very weak peaks in our HRNPD patterns (inset of Fig. 1b). The onset of antiferromagnetism in YCrO_3 is responsible for a kink around 142 K in our magnetization curves (data not shown here)²⁴. As a result, we only show magnetization data measured below 120 K in this paper.

III. RESULTS AND DISCUSSION

We first discuss the bond ordered compound $\text{Y}_2\text{Mn}_2\text{O}_7$ ($x = 0$). The predominant Mn-Mn exchange is ferromagnetic, as evidenced by $\Theta_{\text{CW}} = 41(2)$ K²⁸. The effective magnetic moment (M_{eff}) deduced from fitting the magnetization versus temperature (M - T) curve in the paramagnetic region is $3.84(2) \mu_B/\text{Mn}$, indicating $J = S = 3/2$ for Mn^{4+} (J and S are the total and spin angular momenta,

TABLE I. Structural parameters of $\text{Y}_2\text{Mn}_2\text{O}_7$ (from Ref. 27), Y_2CrSbO_7 and $\text{Y}_2\text{Cr}_{0.4}\text{Ga}_{0.6}\text{SbO}_7$, in which B represents the atomic positions of Mn/Cr/Sb/Ga. The corresponding diffraction patterns were refined under space group $F d -3 m$ ($a = b = c$, $\alpha = \beta = \gamma = 90^\circ$). The only atomic position that needs to be refined is O2 (x , 0.125, 0.125).

	a (Å)	x (O2)	B_{iso} (Å ²)				B -O2 (Å)	B - B (Å)	B -O2- B (°)
			Y	B	O1	O2			
$\text{Y}_2\text{Mn}_2\text{O}_7$ (RT)	9.902(1)	0.3274(8)	0.3(1)	0.1(1)	0.1(3)	0.2(1)	1.911(3)	3.5009(3)	132.7(5)
Y_2CrSbO_7 (300 K)	10.1620(1)	0.4178(1)	0.72(1)	0.44(2)	0.15(3)	0.45(1)	1.9810(6)	3.59282(3)	130.14(2)
Y_2CrSbO_7 (2.0 K)	10.1523(7)	0.41793(8)	0.69(1)	0.34(1)	0.17(2)	0.439(8)	1.9787(3)	3.5894(2)	130.19(1)
$\text{Y}_2\text{Cr}_{0.4}\text{Ga}_{0.6}\text{SbO}_7$ (2.0 K)	10.1508(8)	0.4182(1)	0.58(1)	0.51(2)	0.17(3)	0.37(1)	1.9774(5)	3.58885(2)	130.31(2)

respectively)²⁸. The orbital quenching in $\text{Y}_2\text{Mn}_2\text{O}_7$ is also confirmed by its saturation moment measured at 5 K: $M_s \approx 3.0 \mu_B/\text{Mn}$ ²³. The magnetic ground state of $\text{Y}_2\text{Mn}_2\text{O}_7$ is very sample dependent. Shimakawa *et al.* claim ferromagnetism in their sample based on the λ heat capacity anomaly around 15 K, below which the M - T curve plateaus²³. However, the λ anomaly in heat capacity is not observed in the samples prepared by Reimers *et al.*²⁸ and Greedan *et al.*²⁹. Instead, their results strongly support a SG-like state at low temperatures. The strong sample dependence of magnetic properties might be related to the valence disorder in $\text{Y}_2\text{Mn}_2\text{O}_7$, where high pressure synthesis is required to stabilize Mn^{4+} ^{23,28,30}.

While Cr^{4+} -based pyrochlores also require high pressure synthesis³⁰, Cr^{3+} -based pyrochlores can be prepared at ambient pressure²⁴. To avoid the potential complication to the magnetic structure caused by valence disorder, we have chosen to study the Cr^{3+} -based pyrochlore Y_2CrSbO_7 , where Sb^{5+} is used to compensate the valence loss. Cr^{3+} shares the same $3d^3$ electronic configuration as Mn^{4+} . Moreover, the lattice parameters of Y_2CrSbO_7 are analogous to those of $\text{Y}_2\text{Mn}_2\text{O}_7$ (Table I)²⁷. As a result, the magnetic interactions in the two systems are expected to be similar. Deviation from paramagnetism can be observed in Y_2CrSbO_7 at low temperatures, as revealed by the inverse magnetization versus temperature ($1/M$ - T) curve, (Fig. 1a). A linear fit to the $1/M$ - T curve in the paramagnetic region gives $\Theta_{\text{CW}} = 20.1(6)$ K and $M_{\text{eff}} = 3.99(1) \mu_B/\text{Cr}$. Since Θ_{CW} is proportional to number of magnetic sites per unit cell \times exchange strength³¹, the Cr-Cr and Mn-Mn exchange strengths are very similar to each other in Y_2CrSbO_7 and $\text{Y}_2\text{Mn}_2\text{O}_7$. The M - T curve is also displayed in Fig. 1a. Surprisingly, no ferromagnetism can be observed down to 1.8 K for Y_2CrSbO_7 . The absence of magnetic long range order in Y_2CrSbO_7 is further confirmed by our HRNPD pattern at 2 K, which can be refined by a single crystallographic phase (Fig. 1b).

Within the resolution of our Rietveld refinement ($\sim 1\%$), the Cr:Sb ratio is 1:1 in Y_2CrSbO_7 . Based on Ref. 22, nonmagnetic sites percolate at $x_s \approx 0.61$ on a pyrochlore lattice. Thus, the Cr-sites in Y_2CrSbO_7 ($x = 0.5$) are still percolative with a fraction $f_M = 83(2)\%$ (see Fig. 2c obtained from our simulations, details of which will be discussed below). For a ferromagnetic TM pyrochlore, magnetic frustration is often negligible due to

the lack of possible sources. The expected ferromagnetically ordered moment (M_{exp}) in Y_2CrSbO_7 can be estimated to be $0.83 \times gJ \sim 2.59 \mu_B/\text{Cr}$, where the Landé g -factor is approximately 2 and $J = 1.56$ is extracted from M_{eff} . M_{exp} is well above the resolution of our HRNPD measurements ($< 0.5 \mu_B$). The magnetic frustration in Y_2CrSbO_7 is reflected by the frustration index, $h = \left| \frac{\Theta_{\text{CW}}}{T_t} \right| > 10$, where T_t is the transition temperature. h is 2.7 in $\text{Y}_2\text{Mn}_2\text{O}_7$ and close to 1 in non-frustrated magnets. This high level of frustration is usually not expected for ferromagnetically coupled spins. One possible origin for the suppressed T_t in Y_2CrSbO_7 is nonmagnetic site-disorder. The critical concentration where the magnetic long range order disappears is very close, if not equal, to $x_s \approx 0.61$ ³²⁻³⁵, meaning conventional ferromagnetism should still develop in Y_2CrSbO_7 ($x = 0.5$) below 1.8 K. However, M - T curves in the high field region do not support this scenario (Fig. 3). These magnetic fields are expected to smooth out the ferromagnetic phase transition and leave T_t unchanged³¹.

When diluting the magnetic sites by nonmagnetic ions, bond-disorder is also introduced to the local lattice due to the inevitable ionic size mismatch between M and N . As a result, there will be five types of M/N -tetrahedron in $\text{Y}_2(M_{1-x}N_x)_2\text{O}_7$, which can be labelled as empty, single, double, triple, and full in terms of M occupation (Fig. 2a). For site percolation, bond-disorder is ignored so that the percolation of doubly, triply, and fully occupied tetrahedra are calculated simultaneously. For the bond percolation, on the other hand, bond-disorder is the focus. Bond-disorder will randomly distort the local TMO_6 -octahedron, frustrating the crystal field. Moreover, the random distribution of M -O- M bond angles caused by bond-disorder will lead to exchange fluctuations. Similar effects have been intensively studied in the SG pyrochlore $\text{Y}_2\text{Mo}_2\text{O}_7$, where the Mo-Mo exchange is antiferromagnetic and bond-disorder comes from orbital frustration^{14,15,36,37}.

To qualitatively elucidate the effect of bond-disorder, we have simulated the percolation processes of Cr-sites with at least two (site percolation), three, four, five, and six (bond percolation) nearest neighbour Cr-sites, respectively. The simulations were performed on a $D \times D \times D$ ($D = 48, 64$) cubic pyrochlore lattice (edge-sharing tetrahedral network). This lattice, initially with all sites oc-

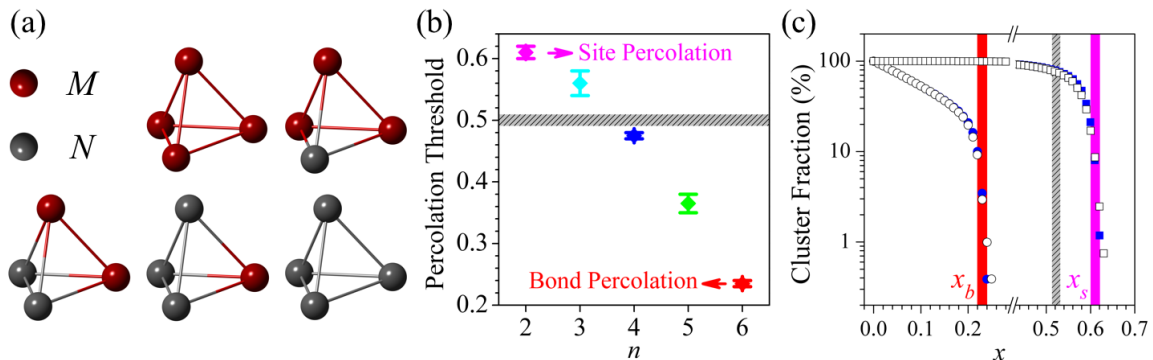


FIG. 2. (a) Five possible configurations of a M/N -tetrahedron. (b) The percolation thresholds produced by our simulations on a $D \times D \times D$ pyrochlore lattice with s sampling times of bond-disorder (red, $D = 64$ and $s = 100$), Cr-clusters with at least five (green, $D = 64$ and $s = 16$), four (blue, $D = 48$ and $s = 16$), three (cyan, $D = 48$ and $s = 16$) nearest neighbour Cr-sites, and site-disorder (magenta, $D = 64$ and $s = 50$). (c) The evolution of the fraction of percolative bond- (circles) and site- (squares) ordered clusters as a function of the nonmagnetic fraction x (blue closed: $D = 48$, black open: $D = 64$). The red (magenta) area marks the percolation region of bond- (site-) disorder. The grey hatched areas in (b) and (c) mark the position of Y_2CrSbO_7 with $\Delta x = 0.01$.

cupied by magnetic ions ($x = 0$), were randomly diluted by nonmagnetic ions to the required composition x . For each composition, the percolation probability is 1 if at least one percolative path is found between any of the two parallel facets of the cube in our simulations. The simulations for each x were sampled by s times. As shown in Fig. 2b, the site percolation threshold, $x_s = 0.61(1)$, produced by our simulations is consistent with the previous study²². In addition, our simulations also predict that bond percolation occurs well ahead of site percolation at $x_b = 0.23(1)$ (Fig. 2b). Due to the valence constraint, we are unable to check x_b in our samples, $Y_2(Cr_{1-x}Ga_{x-0.5}Sb_{0.5})_2O_7$ ($0.5 \leq x \leq 0.9$). However, we have identified a spinel system, $Zn(Cr_{1-x}Ga_x)_2O_4$, where the Cr/Ga-sites form a pyrochlore sublattice. The clean compound $ZnCr_2O_4$ ($x = 0$) undergoes a spin-Peierls-like phase transition at $T_N = 12.5$ K³⁸. By increasing the nonmagnetic Ga fraction (x) on Cr-sites, the magnetically ordered moment drops rapidly to zero; a Néel to SG transition sets in between 0.2 and 0.25²¹. These results are in excellent agreement with our bond percolation model (Fig. 2). The transition temperatures of both Néel order and SG decrease monotonously as a function of x in $Zn(Cr_{1-x}Ga_x)_2O_4$ ²¹. This suggests that Y_2CrSbO_7 might undergo a transition at very low temperatures. Theoretically, bond-disorder is responsible for the onset of the SG state in $Zn(Cr_{1-x}Ga_x)_2O_4$ ^{14,15}. While the magnetic ground state of Y_2CrSbO_7 is not experimentally confirmed yet, it is likely that it is also a SG caused by bond-disorder.

The ionic radii of Cr^{3+} , Ga^{3+} , and Sb^{5+} are 0.615 Å, 0.62 Å, and 0.60 Å, respectively³⁹. As a result, the strength of bond-disorder in this system is very weak, but still sufficient to see an effect. Advanced SG theories, which can be applied to $Zn(Cr_{1-x}Ga_x)_2O_4$ and $Y_2Mo_2O_7$, have demonstrated a spin freezing transition in the zero bond-disorder limit. To estimate the strength

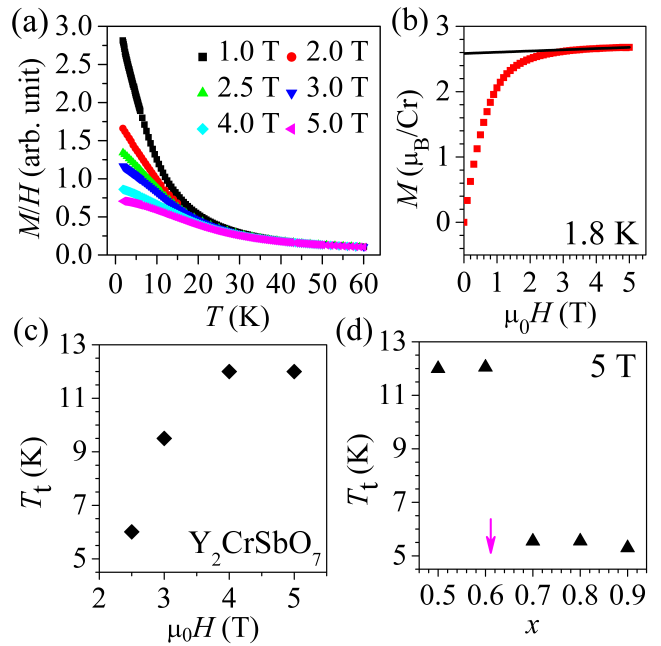


FIG. 3. (a) Susceptibility (M/H) of Y_2CrSbO_7 versus temperature curves in the high field region. (b) Field scan of the magnetization of Y_2CrSbO_7 at 1.8 K. The black line is a linear fit to the data above 3.5 T. (c) Magnetic field dependence of the transition temperature (T_t) in Y_2CrSbO_7 . (d) x -dependence of T_t measured at 5 T, showing the recovery of site percolation. The vertical arrow marks the position of x_s .

of bond-disorder in $Y_2(Cr_{1-x}Ga_{x-0.5}Sb_{0.5})_2O_7$, we examine the magnetic properties under an external perturbation, i.e. magnetic field. As shown in Fig. 3a, a low temperature magnetization plateau gradually develops in Y_2CrSbO_7 as magnetic field is increased. The field-dependence of the magnetization is displayed in Fig. 3b.

The magnetization is saturated between 3.0 and 4.0 T with $M_s = 2.59 \mu_B/\text{Cr} = M_{\text{exp}}$. This may suggest that only the spins on percolative Cr-sites are ordered. The transition temperature T_t is defined as the point where the corresponding M - T curve has the steepest slope. The continuous increase of T_t as a function of magnetic field ($\mu_0 H < 4$ T) supports the idea of a highly frustrated zero-field magnetic ground state with nonuniform bond-disorder. At 4 T and above, T_t of Y_2CrSbO_7 tends to saturate ~ 12 K (Fig. 3c). This deviates from the behaviour of a polarized paramagnet³¹. We note that T_t only saturates when the percolative Cr-spins are fully aligned. In other words, magnetic long range order is fully recovered in Y_2CrSbO_7 when the magnetic frustration is removed. As a result, the strength of bond-disorder in Y_2CrSbO_7 is estimated to range from 0 T and 3.5 T. A sudden drop in T_t measured at 5 T is observed between 0.6 and 0.7 (Fig. 3d). It means that long range spin correlation, which is recovered by suppressing the magnetic frustration caused by bond-disorder, develops in the high field region for $x < x_s = 0.61(1)$. It also indicates that our samples are stoichiometrically homogeneous with $\Delta x < 0.02$.

IV. SUMMARY

Based on our magnetization and HRNPD measurements (Fig. 1), we have observed a very high level of magnetic frustration ($h > 10$) in the TM pyrochlore Y_2CrSbO_7 where the Cr-Cr exchange is predominantly ferromagnetic. The magnetic frustration cannot be explained by nonmagnetic site-disorder (Sb). We propose percolative bond-disorder caused by the ionic size mismatch as the driving mechanism. The average Cr/Sb-O-Cr/Sb bond angle is $130.19(1)$ degrees in Y_2CrSbO_7 . Based on a previous study on the Cr-based oxides with

very similar lattice parameters, this value is in the critical region where the Cr-Cr exchange interaction changes its sign⁴⁰. Because of this, zero point exchange fluctuations might be present although the overall exchange is ferromagnetic. Secondly, bond-disorder will also affect the local crystal field environment, e.g. frustrating the single-ion anisotropy. We have also estimated the strength of bond-disorder in Y_2CrSbO_7 , which is in the region of [0 T, 3.5 T]. As a result, both magnetic long range order and site percolation process can be recovered by applying high magnetic fields (Fig. 3).

For $\text{Y}_2(M_{1-x}N_x)_2\text{O}_7$ (M = magnetic TM ion, N = nonmagnetic ion), we have performed numerical simulations to study the percolation process of various clusters, including bond-, site-disorder, and several intermediate states in between. Our results unambiguously reveal that bond-disorder [$x_b = 0.23(1)$] percolates well ahead of site-disorder [$x_s = 0.61(1)$]. More importantly, our model can be experimentally verified in the spinel system $\text{Zn}(\text{Cr}_{1-x}\text{Ga}_x)_2\text{O}_4$ where a Néel to SG transition can be induced by Ga-substitution (Fig. 2)²¹. Considering the similarity between the Cr/Sb- and Cr/Ga- sublattices in many aspects, we propose that the magnetic ground state of Y_2CrSbO_7 is a SG. We also call for further investigations in future. For example, experiments, e.g. heat capacity and HRNPD, in the ultra-low temperature region (< 1.8 K) would be helpful to understand the magnetic ground state of Y_2CrSbO_7 . Investigations on the local crystallographic structure are needed to check the amplitude of exchange fluctuations.

ACKNOWLEDGMENTS

We thank M. W. Long and E. M. Forgan for helpful discussions. We acknowledge the UK EPSRC for funding under grant number EP/J016977/1.

¹ H. T. Diep, *Frustrated Spin Systems*, 2nd ed. (World Scientific, 2013).
² J. S. Gardner, M. J. P. Gingras, and J. E. Greedan, *Rev. Mod. Phys.* **82**, 53 (2010).
³ R. Moessner and J. T. Chalker, *Phys. Rev. Lett.* **80**, 2929 (1998).
⁴ R. Moessner and J. T. Chalker, *Phys. Rev. B* **58**, 12049 (1998).
⁵ B. Canals and C. Lacroix, *Phys. Rev. Lett.* **80**, 2933 (1998).
⁶ M. J. Harris, S. T. Bramwell, D. F. McMorrow, T. Zeiske, and K. W. Godfrey, *Phys. Rev. Lett.* **79**, 2554 (1997).
⁷ S. T. Bramwell and M. J. P. Gingras, *Science* **294**, 1495 (2001).
⁸ D. J. P. Morris, D. A. Tennant, S. A. Grigera, B. Klemke, C. Castelnovo, R. Moessner, C. Czternasty, M. Meissner, K. C. Rule, J.-U. Hoffmann, K. Kiefer, S. Gerischer, D. Slobinsky, and R. S. Perry, *Nature* **326**, 411 (2009).
⁹ C. Castelnovo, R. Moessner, and S. L. Sondhi, *Nature*

451, 42 (2008).
¹⁰ K. Binder and A. P. Young, *Rev. Mod. Phys.* **58**, 801 (1986).
¹¹ S. Nagata, P. H. Keesom, and H. R. Harrison, *Phys. Rev. B* **19**, 1633 (1979).
¹² A. Morgownik and J. Mydosh, *Solid State Communications* **47**, 321 (1983).
¹³ H. Maletta and W. Felsch, *Phys. Rev. B* **20**, 1245 (1979).
¹⁴ T. E. Saunders and J. T. Chalker, *Phys. Rev. Lett.* **98**, 157201 (2007).
¹⁵ H. Shinaoka, Y. Tomita, and Y. Motome, *Phys. Rev. Lett.* **107**, 047204 (2011).
¹⁶ M. J. P. Gingras, C. V. Stager, N. P. Raju, B. D. Gaulin, and J. E. Greedan, *Phys. Rev. Lett.* **78**, 947 (1997).
¹⁷ K. Miyoshi, Y. Nishimura, K. Honda, K. Fujiwara, and J. Takeuchi, *Journal of the Physical Society of Japan* **69**, 3517 (2000).
¹⁸ J. Greedan, M. Sato, X. Yan, and F. Razavi, *Solid State Communications* **59**, 895 (1986).

- ¹⁹ W. Ratcliff, S.-H. Lee, C. Broholm, S.-W. Cheong, and Q. Huang, *Phys. Rev. B* **65**, 220406 (2002).
- ²⁰ D. Fiorani, S. Viticoli, J. L. Dormann, J. L. Tholence, and A. P. Murani, *Phys. Rev. B* **30**, 2776 (1984).
- ²¹ S.-H. Lee, W. Ratcliff, Q. Huang, T. H. Kim, and S.-W. Cheong, *Phys. Rev. B* **77**, 014405 (2008).
- ²² C. L. Henley, *Canadian Journal of Physics* **79**, 1307 (2001).
- ²³ Y. Shimakawa, Y. Kubo, N. Hamada, J. D. Jorgensen, Z. Hu, S. Short, M. Nohara, and H. Takagi, *Phys. Rev. B* **59**, 1249 (1999).
- ²⁴ M. J. Whitaker and C. Greaves, *Journal of Solid State Chemistry* **215**, 171 (2014).
- ²⁵ L. Shen, E. Blackburn, T. Hansen, and R. Riyat, *Field induced long range magnetic order and percolation transition in $Y_2Cr_{1-x}Ga_xSbO_7$* (2014), Institut Laue-Langevin (ILL) doi:10.5291/ILL-DATA.5-31-2332.
- ²⁶ J. Rodríguez-Carvajal, *Physica B: Condensed Matter* **192**, 55 (1993).
- ²⁷ M. Subramanian, C. Torardi, D. Johnson, J. Pannetier, and A. Sleight, *Journal of Solid State Chemistry* **72**, 24 (1988).
- ²⁸ J. N. Reimers, J. E. Greedan, R. K. Kremer, E. Gmelin, and M. A. Subramanian, *Phys. Rev. B* **43**, 3387 (1991).
- ²⁹ J. E. Greedan, N. P. Raju, A. Maignan, C. Simon, J. S. Pedersen, A. M. Niraimathi, E. Gmelin, and M. A. Subramanian, *Phys. Rev. B* **54**, 7189 (1996).
- ³⁰ H. Fujinaka, N. Kinomura, M. Koizumi, Y. Miyamoto, and S. Kume, *Materials Research Bulletin* **14**, 1133 (1979).
- ³¹ S. Blundell, *Magnetism in Condensed Matter* (Oxford University Press, 2011).
- ³² S.-W. Cheong, A. S. Cooper, L. W. Rupp, B. Batlogg, J. D. Thompson, and Z. Fisk, *Phys. Rev. B* **44**, 9739 (1991).
- ³³ D. J. Breed, K. Gilijamse, J. W. E. Sterkenburg, and A. R. Miedema, *Journal of Applied Physics* **41**, 1267 (1970).
- ³⁴ D. Kumar and A. B. Harris, *Phys. Rev. B* **8**, 2166 (1973).
- ³⁵ R. A. Tahir-Kheli, T. Fujiwara, and R. J. Elliott, *Journal of Physics C: Solid State Physics* **11**, 497 (1978).
- ³⁶ J. A. Paddison and et al, arXiv:1506.05045 (2015).
- ³⁷ J. E. Greedan, D. Gout, A. D. Lozano-Gorrin, S. Derahkshan, T. Proffen, H.-J. Kim, E. Božin, and S. J. L. Billinge, *Phys. Rev. B* **79**, 014427 (2009).
- ³⁸ S.-H. Lee, C. Broholm, T. H. Kim, W. Ratcliff, and S.-W. Cheong, *Phys. Rev. Lett.* **84**, 3718 (2000).
- ³⁹ R. D. Shannon, *Acta Crystallographica Section A* **32**, 751 (1976).
- ⁴⁰ K. Motida and S. Miyahara, *Journal of the Physical Society of Japan* **28**, 1188 (1970).